Electronic Supplementary Information for

Machine Learning Protocol for Revealing Ion Transport Mechanisms from Dynamic NMR Shifts in Paramagnetic Battery Materials

Min Lin,[a] Jingfang Xiong,[a] Mintao Su,[a] Feng Wang,[a] Xiangsi Liu,[a] Yifan Hou,[a] Riqiang Fu,[d] Yong Yang*[ab] and Jun Cheng*[ac]

[a] Collaborative Innovation Center of Chemistry for Energy Materials, State Key Laboratory for Physical Chemistry of Solid Surface, College of Chemistry and Chemical Engineering, Xiamen University, Xiamen 361005, China.

[b] College of Energy, Xiamen University, Xiamen 361005, China.

[c] Innovation Laboratory for Sciences and Technologies of Energy Materials of Fujian Province (IKKEM), Xiamen 361005, China.

[d] National High Magnetic Field Laboratory 1800 E. Paul Dirac Drive, Tallahassee, Florida 32310 (USA).

E-mail: yyang@xmu.edu.cn (Yong Yang); chengjun@xmu.edu.cn (Jun Cheng)

Supplementary methods

Magnetic Susceptibility. The magnetic susceptibility of P2-type $Na_{2/3}(Ni_{1/3}Mn_{2/3})O_2$ was measured by a superconducting quantum interference device (SQUID) magnetometer within 2–390 K at 100 Oe and field-cooled (FC) condition.

^{23}Na magic-angle spinning (MAS) NMR spectra. The ^{23}Na MAS NMR spectrum of P2-$Na_{2/3}(Ni_{1/3}Mn_{2/3})O_2$ was acquired on Bruker Avance III 400 MHz NMR spectrometer using a 1.3 mm double-resonance HX probe with a spinning speed of 50 kHz. A Hahn-echo pulse sequence (90° pulse – τ – 180° pulse – τ) was adopted, in which the 90° and 180° pulse lengths were 1.0 and 2.0 μs, respectively. 40960 scans were accumulated with a recycle delay of 0.01 ms. The ^{23}Na chemical shift was referenced to 1M NaCl aqueous solution at 0 ppm.

Experimental powered X-ray diffraction (PXRD) spectra. The PXRD spectra of P2-$Na_{2/3}(Ni_{1/3}Mn_{2/3})O_2$ were collected on a SmartLab-SE powder X-ray diffractometer using Cu Kα radiation (λ = 1.5406 Å), in which voltage and current is 40 kV and 30 mA, respectively, and the probe works from10° to 80° at a scanning rate of 2° 2θ/min. The PXRD spectra were refined using the *FullProf*[1] program with the spacegroup $P6_3/mmc$.

Simulation of PXRD spectra. The simulation of $P6_3/mcm$-$P6_322$ (P2) and $P6_322$-$P6_3mc$ (P2-O2) mixed stacking PXRD spectra were performed with *FAULTS* program[2], in which recursive stacking sequences alone (002) direction define the stacking models of $Na_{2/3}(Ni_{1/3}Mn_{2/3})O_2$ layer by layer. We defined two distinct original layers for P2 mixed stacking models, and four distinct original layers for P2-O2 mixed stacking models. The atomic coordinates were extracted from the above-mentioned *FullProf*[1] refinement results. For the O2 phase, the DFT method optimized cell parameters were applied to define the transition vector alone *z*-axis. The crystal models were fully randomly built upon stacking probabilities. To eliminate the finite size line broadening effect, the number of stacking sequence large than 1022 was utilized[2], peak broadening parameters and scale factors keep the same in all PXRD simulations.

Calculation of Na diffusion coefficient (D_{Na}). The mean-squared displacement of Na$^+$ ($MSD_{Na}(t)$) is given by[3,4]:

$$MSD_{Na}(t) = \frac{1}{N}\sum_{i=1}^{N}\left(\left[r_i(t+t_0)\right] - \left[r_i(t_0)\right]\right)^2 \qquad (1)$$

Where $r_i(t+t_0)$ is the displacement of single Na$^+$ during simulation time t with respect to the start position $r_i(t_0)$, N is the number of Na$^+$ and t_0 is starting simulation time. Na$^+$ diffusion coefficients (D_{Na}) were estimated by the slope of linear fitting of MSD over time interval t:

$$D_{Na} = \frac{MSD_{Na}(t)}{2d \cdot t} \qquad (2)$$

Where d is the number of diffusion dimensions.

Simulation of time-averaged NMR spectra of ^{23}Na shifts (δ_{NN}). Firstly, every 200 ns DPMD trajectory was divided sequentially and equally into short trajectories. Then, the averaged ^{23}Na shift of each Na$^+$ was calculated for each short trajectory. Finally, all averaged ^{23}Na shifts with a Gaussian broadening (σ = 50 ppm) of short trajectories were superposed to simulate total time-averaged ^{23}Na spectra. Lengths of time of short trajectories vary from 4 ps to 200 ns. To clarify the simulated averaged ^{23}Na spectra, their intensities were normalized in each subfigure (Figure S11) according to the No. of time-averaged ^{23}Na shifts.

Supplementary Figures

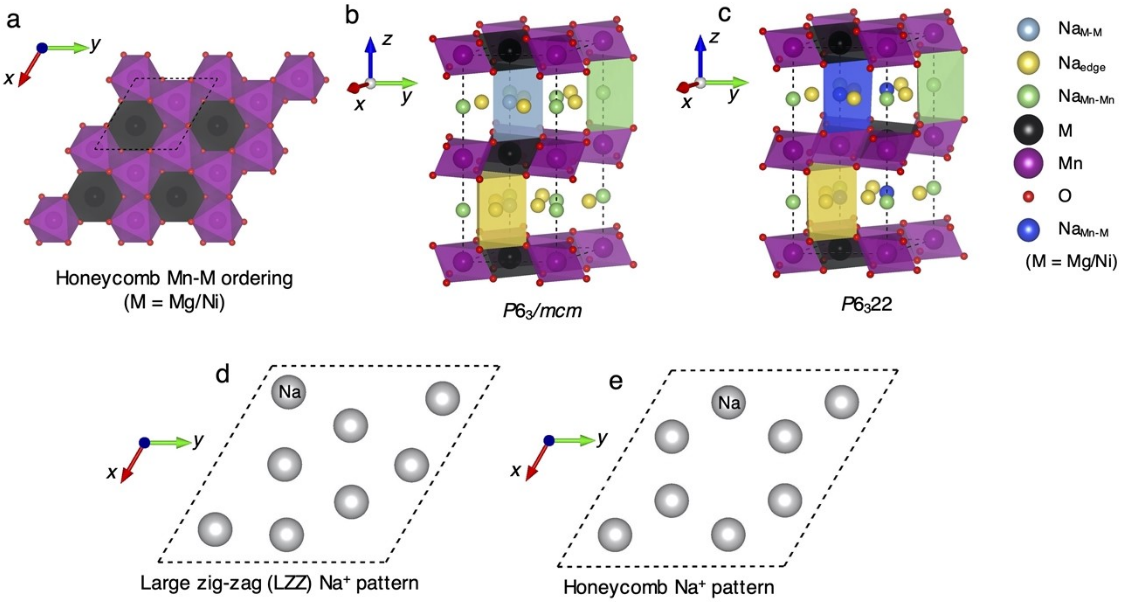

Figure S1. (a, b, c) Crystal structures of P2-type $Na_{2/3}(M_{1/3}Mn_{2/3})O_2$ (M=Mg/Ni). The superstructure and space group were labeled, and the black dotted lines indicate unit cells. For clarification, only one prism of each distinct site was shown in unit cells. (c) LZZ and (b) honeycomb Na^+ patterns. The black dotted lines indicate $2 \times 2 \times 1$ supercells.

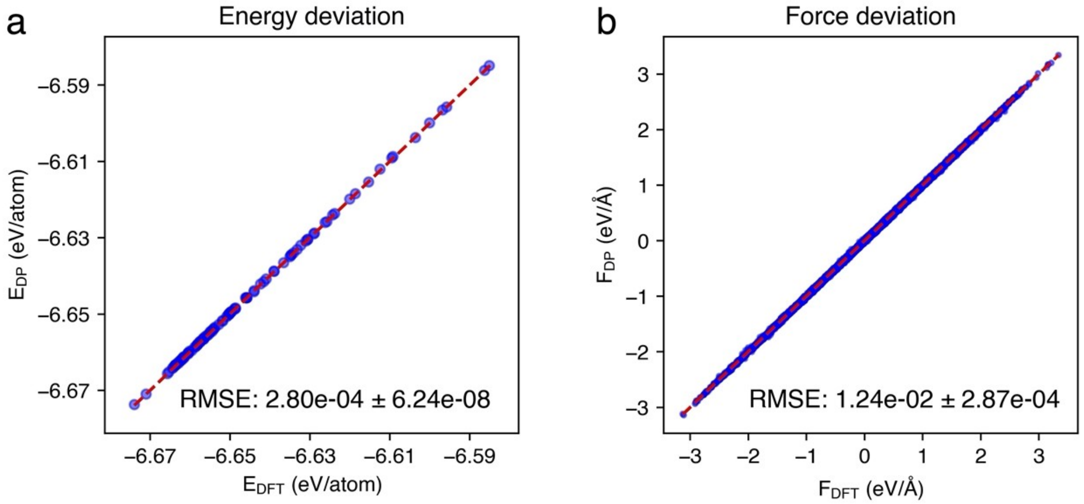

Figure S2. The (a) energy and (b) force correlation between DFT and final deep potential (DP) model of P2-type $Na_{2/3}(Ni_{1/3}Mn_{2/3})O_2$, dashed red lines indicate perfect correlations. The root-mean-square errors (RMSE) and their standard deviations were labeled in each figure.

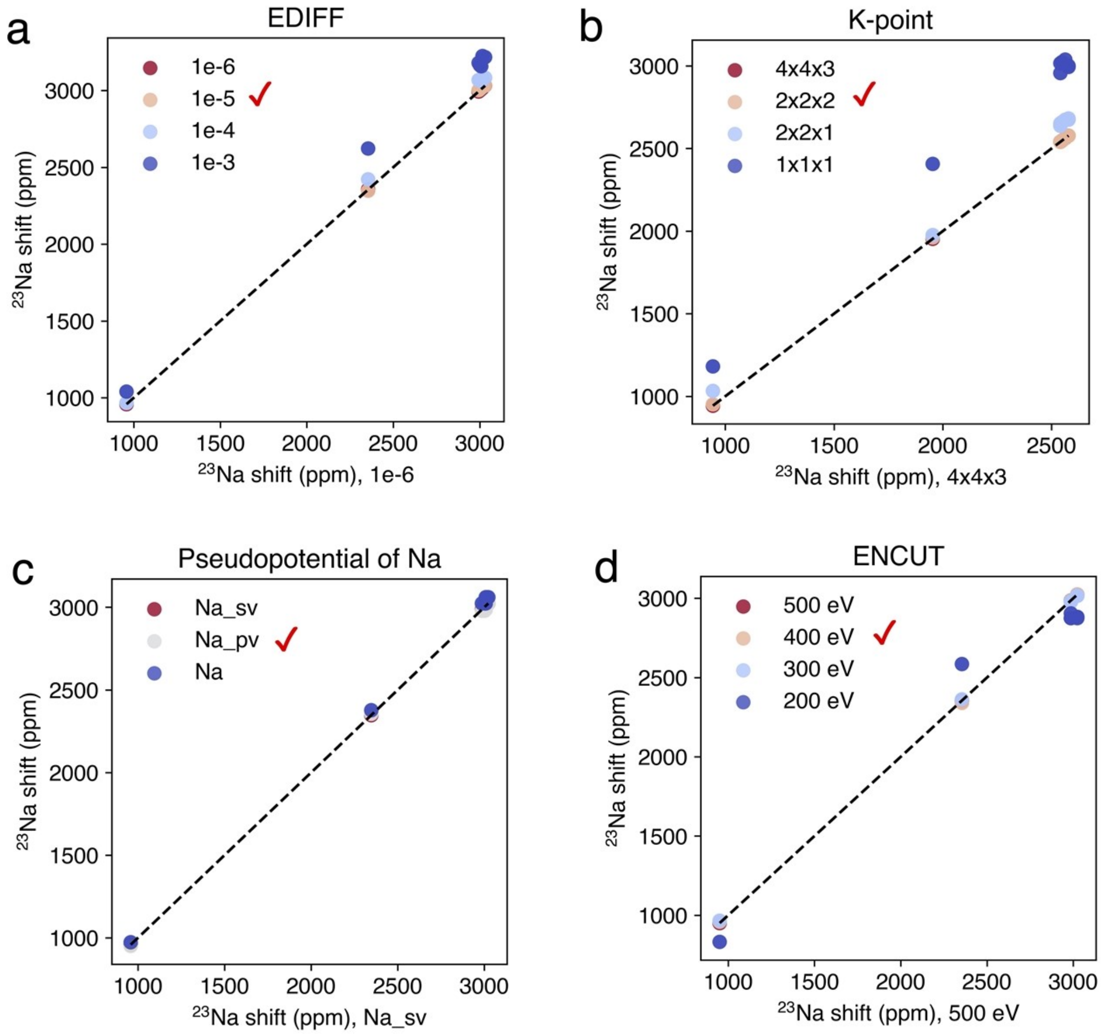

Figure S3. The convergence of ^{23}Na shift of $P6_3/mcm$ $\mathrm{Na_{2/3}(Mg_{1/3}Mn_{2/3})O_2}$ calculated using VASP software and the LZZ Na$^+$ pattern. (a) Convergence criterion of SCF iterations, (b) K-point sampling, (c) pseudopotential of Na, (d) plane wave energy cutoff. Dashed black lines indicate perfect correlations. The final choices were labeled in red ‘√’.

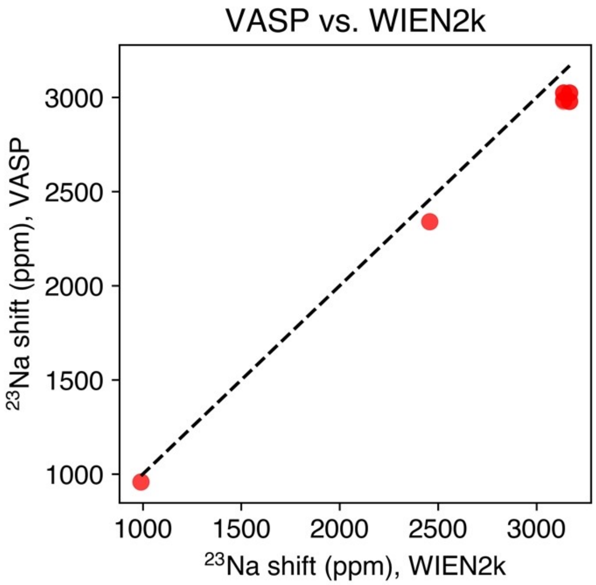

Figure S4. Comparison of $P6_3/mcm$ $Na_{2/3}(Mg_{1/3}Mn_{2/3})O_2$ ^{23}Na shift calculated with WIEN2k and with VASP. The dashed black line indicates a perfect correlation.

Systematic convergence tests of ^{23}Na shift of $P6_3/mcm$ $Na_{2/3}(Mg_{1/3}Mn_{2/3})O_2$ with PBE functional (Figure S3) were conducted for the convergence criterion of self-consistent field (SCF) iterations, K-point, Na pseudopotential, cut-off energy of plane wave basis set that were determined as 10^{-5} eV, $2 \times 2 \times 2$, *Na_pv*, 400 eV, respectively. Comparing with the ^{23}Na shift calculated with PBE functional and computational setup in our previous work[5] that was implemented in all-electron WIEN2k code[6], the pseudopotential-based VASP code could well reproduce the ^{23}Na shift of $P6_3/mcm$ NMMO (Figure S4). Since all-electron code is more accurate for calculating the spin density at nuclear positions, it is always good to compare the Fermi-contact shift calculated with the VASP code to with all-electron codes.

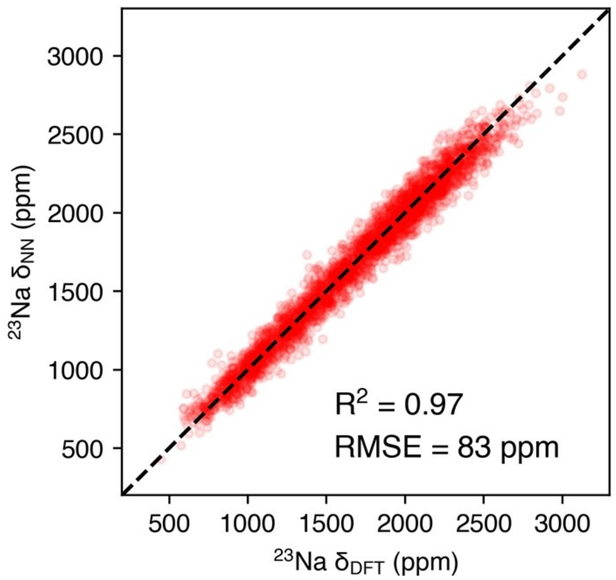

Figure S5. The correlation of P2-type $Na_{2/3}(Ni_{1/3}Mn_{2/3})O_2$ ^{23}Na δ_{DFT} and δ_{NN}, the dashed black line indicates a perfect correlation. The RMSE and R^2 factor were labeled.

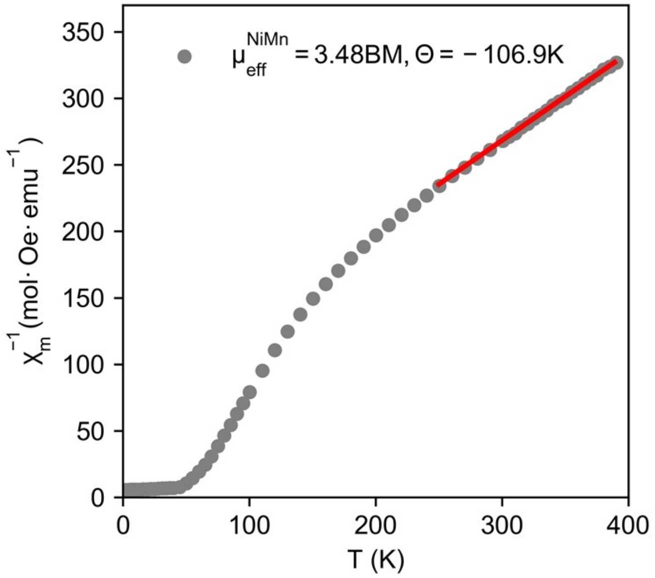

Figure S6. The reciprocal magnetic susceptibility (χ_m^{-1}) of P2-type $Na_{2/3}(Ni_{1/3}Mn_{2/3})O_2$. The red solid line indicates the linear fitting in terms of χ^{-1}= (T–Θ)/C in a temperature range of 250K and 390K. The fitted effective moment μ_{eff} = 3.48μ_B/TM^{4+} and Wiess constant Θ = -106.9 K were labeled. The negative sign of Θ points to predominantly anti-ferromagnetic interactions between Mn^{4+} and Ni^{2+}.

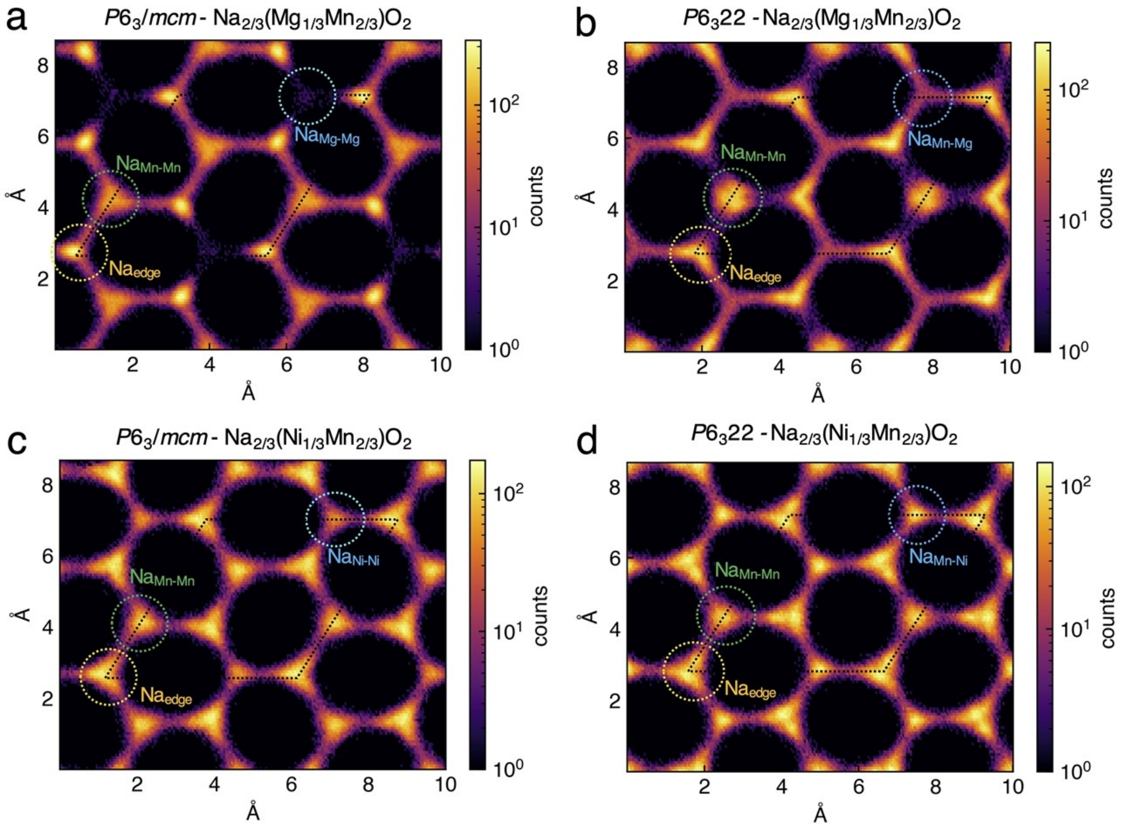

Figure S7. The *xy*-plane Na^+ distribution maps based on 200 ns DPMD simulations at 300 K. The numbers of Na^+ were counted using a time interval of 4 ps and not normalized. The dotted circles and rhombi indicate Na sites and unit cells, respectively.

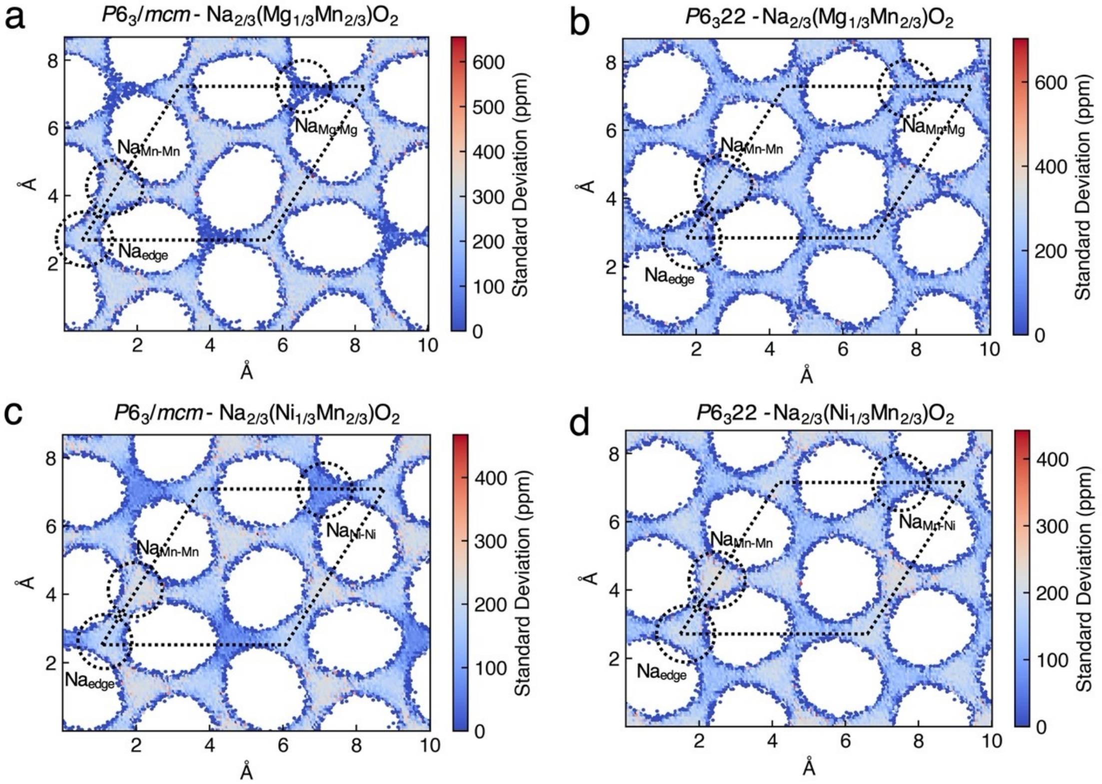

Figure S8. The standard deviation (STD) of ^{23}Na shift of each grid on *xy*-plane. The dotted circles and rhombi indicate Na sites and unit cells, respectively.

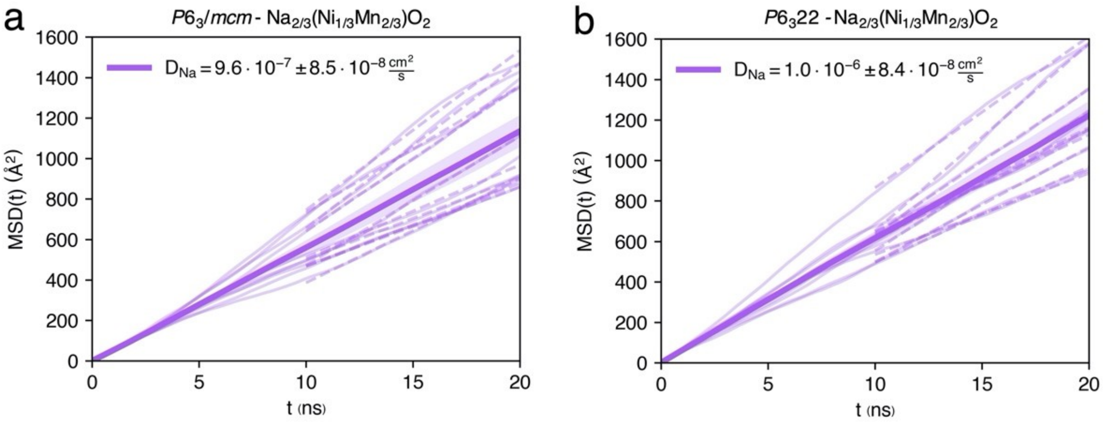

Figure S9. The mean-squared displacement (MSD) of Na^+ in (a) $P6_3/mcm$ and (b) $P6_3/22$ at 300 K with a simulation time of 200 ns. Each 200 ns simulation was truncated into 10 trajectories for analyzing the Na^+ diffusion coefficient (D_{Na}). The thin and thick solid purple lines indicate the MSD of 10 trajectories and their mean values, respectively. The dashed purple lines indicate the linear fitting of MSD during the last 10 ns of truncated trajectories.

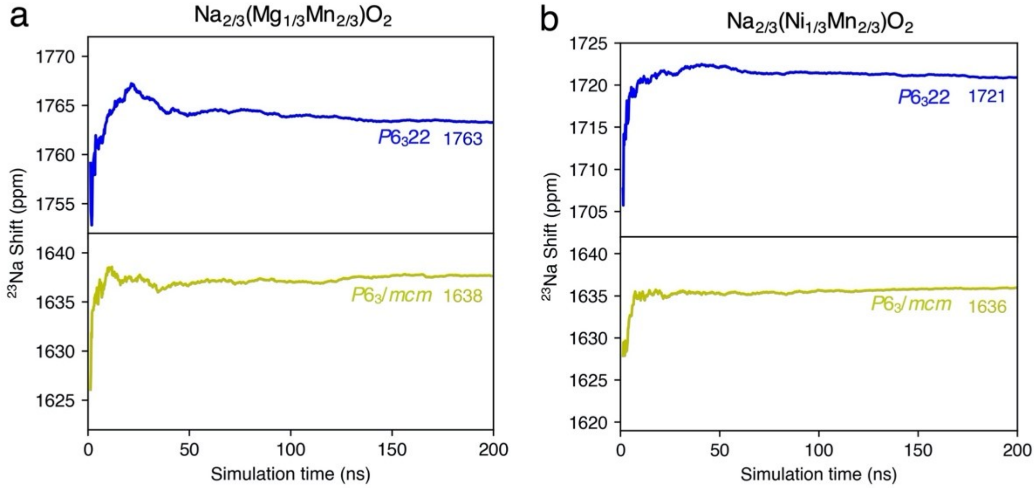

Figure S10. The averaged ^{23}Na δ_{NN} of (a) P2-type $Na_{2/3}(Mg_{1/3}Mn_{2/3})O_2$ and (b) $Na_{2/3}(Ni_{1/3}Mn_{2/3})O_2$ evolves with simulation time. The space group and its averaged ^{23}Na δ_{NN} over 200 ns were labeled in each subfigure.

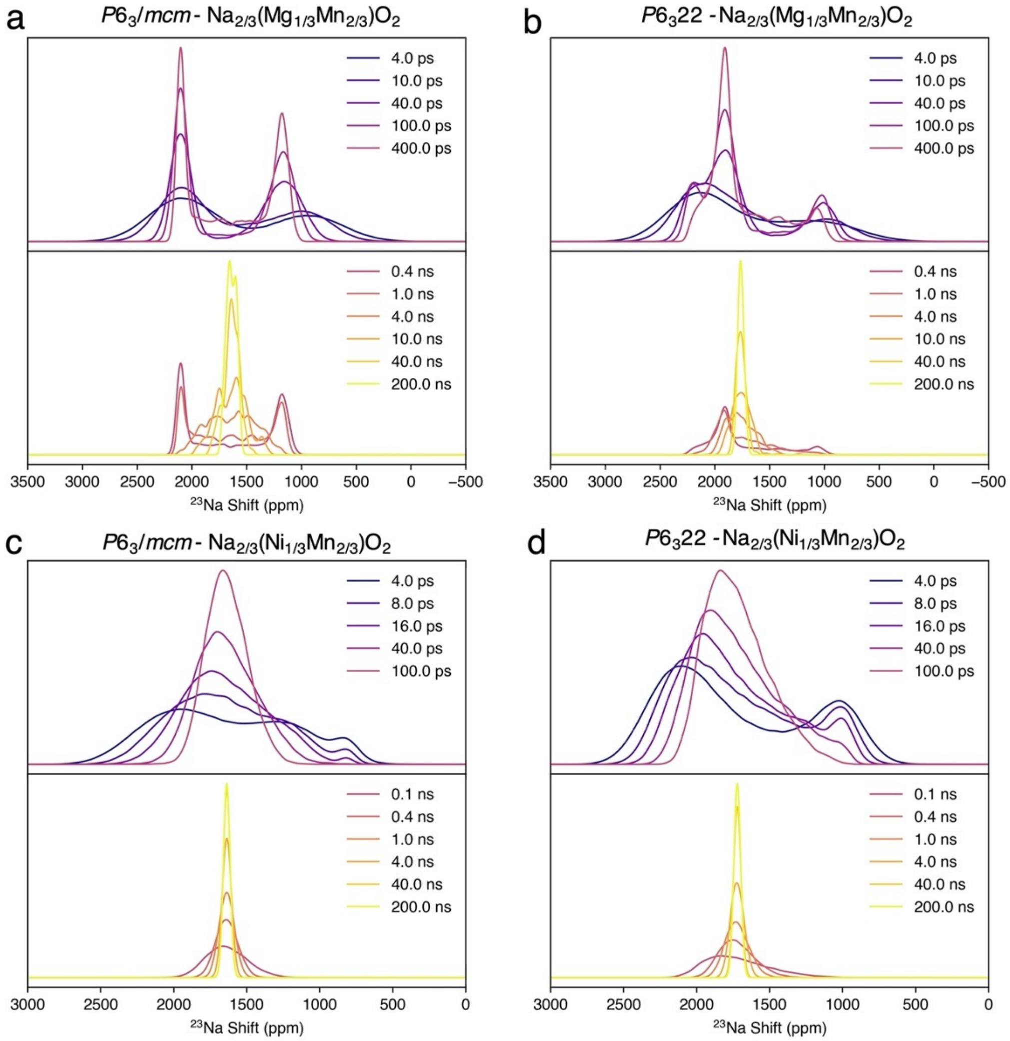

Figure S11. The simulated NMR spectra of ^{23}Na δ_{NN} evolves with averaged periods of time, the corresponding supercell models are labeled. The spectra intensities were normalized in each subfigure according to No. of time-averaged ^{23}Na shifts.

The time-averaged ^{23}Na δ_{NN} spectra with increasing periods of time indicate the formation processes of dynamic NMR spectra (Figure S11). For $P6_3/mcm$ and $P6_322$ NMMO, the ^{23}Na shift peaks become shape from 4 ps to 400 ps, indicating that Na^+ vibrations around Na sites are dominative processes during that period of time; the peaks merge from 400 ps to 200 ns, indicating that Na^+ frequently hop between Na sites. For $P6_3/mcm$ and $P6_322$ NNMO, the periods of time of Na^+ vibration around Na sites are not obvious, indicating a faster Na^+ hopping between Na sites, which agrees with the higher D_{Na} of NNMO than that of NMMO.

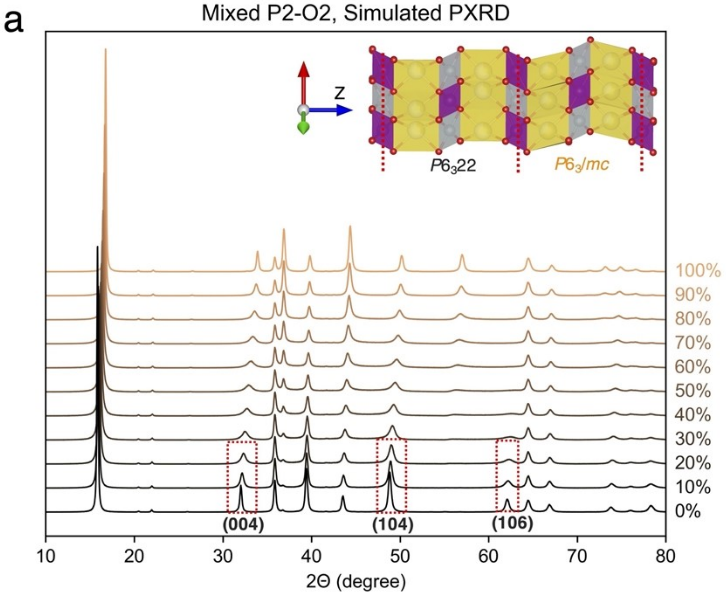

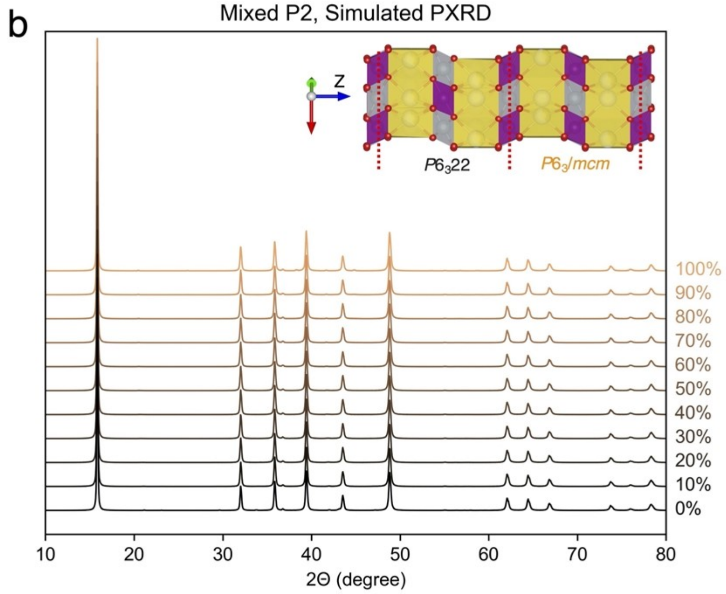

Figure S12. (a) The PXRD spectra of mixed *P*6$_3$22-*P*6$_3$*mc* (P2-O2) $Na_{2/3}(Ni_{1/3}Mn_{2/3})O_2$ vary with the fractions of the space group. (b) The PXPD spectra of mixed stacking *P*6$_3$/*mcm*-*P*6$_3$22 (P2) $Na_{2/3}(Ni_{1/3}Mn_{2/3})O_2$ vary with the fractions of the space group. The structures of mixed stacking were inserted in each figure, and the fractions of *P*6$_3$/*mcm* or *P*6$_3$/*mc* were labeled.

References

1 J. Rodríguez-Carvajal, *Phys. B Condens. Matter*, 1993, **192**, 55–69.

2 M. Casas-Cabanas, M. Reynaud, J. Rikarte, P. Horbach and J. Rodríguez-Carvajal, *J. Appl. Crystallogr.*, 2016, **49**, 2259–2269.

3 L. Kahle, A. Musaelian, N. Marzari and B. Kozinsky, *Phys. Rev. Mater.*, 2019, **3**, 055404.

4 X. He, Y. Zhu, A. Epstein and Y. Mo, *npj Comput. Mater.*, 2018, **4**, 18.

5 M. Lin, X. Liu, Y. Xiang, F. Wang, Y. Liu, R. Fu, J. Cheng and Y. Yang, *Angew. Chemie Int. Ed.*, 2021, **60**, 12547–12553.

6 P. Blaha, K. Schwarz, F. Tran, R. Laskowski, G. K. H. Madsen and L. D. Marks, *J. Chem. Phys.*, 2020, **152**, 074101.